

Critical points of the anyon-Hubbard model

J. Arcila-Forero, R. Franco, and J. Silva-Valencia*

Departamento de Física, Universidad Nacional de Colombia, A. A. 5997 Bogotá, Colombia.

(Dated: March 19, 2019)

Anyons are particles with fractional statistics that exhibit a nontrivial change in the wavefunction under an exchange of particles. Anyons can be considered to be a general category of particles that interpolate between fermions and bosons. We determined the position of the critical points of the one-dimensional anyon-Hubbard model, which was mapped to a modified Bose-Hubbard model where the tunneling depends on the local density and the interchange angle. We studied the latter model by using the density matrix renormalization group method and observed that gapped (Mott insulator) and gapless (superfluid) phases characterized the phase diagram, regardless of the value of the statistical angle. The phase diagram for higher densities was calculated and showed that the Mott lobes increase (decrease) as a function of the statistical angle (global density). The position of the critical point separating the gapped and gapless phases was found using quantum information tools, namely the block von Neumann entropy. We also studied the evolution of the critical point with the global density and the statistical angle and showed that the anyon-Hubbard model with a statistical angle $\theta = \pi/4$ is in the same universality class as the Bose-Hubbard model with two body interactions.

PACS numbers: 05.30.Pr, 37.10.Jk, 05.30.Rt

I. INTRODUCTION

Physicists have proposed a third class of particles with nontrivial exchange statistics, anyons, particles carrying fractional statistics that interpolate between bosons and fermions [1–3]. For two anyons under particle exchange, the wave function acquires a fractional phase $e^{i\theta}$, giving rise to fractional statistics with $0 < \theta < \pi$. Greater interest in the study of anyons emerged when the fractional quantum Hall effect, observed experimentally, had a natural explanation in terms of anyons [4, 5]. Another discovery that reinforced this interest was evidence of superconductor anyon gas [6, 7]. Anyons are very important in numerous studies related to the fractional quantum Hall effect [8, 9], condensed matter physics, and topological quantum computation [10–12]. The study of anyons was restricted for many years to two-dimensional systems. However, with Haldane’s definition of fractional statistics, it was generalized to arbitrary dimensions [3].

One-dimensional (1D) anyons have been studied from different theoretical approaches. Kundu obtained the exact solution of the one-dimensional anyon gas using the generalized coordinate Bethe ansatz method and found the generalized commutation relations for anyons [13]. Furthermore, Batchelor *et al.* showed that the low energies, the dispersion relations, and the generalized exclusion statistics depend on both the anyonic statistical angle and the dynamical interaction parameters in a 1D anyon gas [14]. Alternatively, in tight waveguides, the Fermi-Bose mapping method for one-dimensional Bose and Fermi gases was generalized to an anyon-fermion mapping and applied in order to obtain exact solutions of several models of ultracold gases with anyonic exchange

symmetry [15]. In 2007, Calabrese and Mintchev studied the correlation functions of the 1D anyonic gapless systems in the low-momentum regime [16]. Interesting features appear, including universal oscillating terms with frequency proportional to the statistical parameter and beating effects close to the fermion points. Later, Vitoriano and Coutinho-Filho [17] studied the ground state and low-temperature properties of an integrable Hubbard model with bond-charge interaction, finding that the model displays fractional statistical properties. Remarkably, one-dimensional anyons can be realized as low-energy excitations of the Hubbard model of fermions with correlated hopping processes. On the other hand, Hao *et al.* investigated the ground state [18] and dynamical [19] properties of anyons confined in one-dimensional optical lattices with a weak harmonic trap using an exact numerical method based on a generalized Jordan-Wigner transformation. Also, two-component mixtures of anyons under an external trap were considered by Zinner [20] and the correlation functions of one-dimensional hard-core anyons were calculated by Patu [21].

Note that various experimental proposals for the creation, detection, and manipulation of anyons have been made. Rotating Bose-Einstein condensates have been used to create anyons [22], and the results can be understood in terms of the fractional quantum Hall effect for bosons [23]. This system offers the formation of particles exhibiting fractional statistics with a well-controlled setup that can allow experimentalists to test their fractional statistics. Later on, Duan and colleagues described a general technique for controlling many-body spin Hamiltonians using ultracold atoms, and they showed how to implement an exactly-solvable spin Hamiltonian that supports Abelian and non-Abelian anyonic excitations with exotic fractional statistics [24]. On the other hand, it is possible to use an atomic spin lattice

* jsilvav@unal.edu.co

in optical cavities for the direct measurement of anyonic statistics [25] or trapped atoms in an optical lattice in order to create anyons in topological lattice models. These types of schemes allow the creation of topologically ordered states and detect their statistics [26]. Alternatively, a suggestion has been made for creating anyons on a 1D lattice based on light propagation in an engineered array of optical waveguides. This photonic setup enables us to see the impact of the statistical exchange phase θ on the correlated tunneling dynamics [27]. Furthermore, the possibility of realizing the bosonic fractional quantum Hall effect in ultracold atomic systems has been shown, suggesting a new route to producing and manipulating anyons [28].

We would especially like point out that several proposals for using ultracold bosons to produce anyons in an optical lattice have been made. In particular, Keilmann *et al.* propose a realistic setup for demonstrating an interacting gas of anyons using Raman-assisted hopping in a 1D optical lattice [29]. They introduced the anyon-Hubbard model, which is equivalent to a modified Bose-Hubbard model in which the bosonic hopping depends on the local density. This is an exact mapping between anyons and bosons in one dimension. They found, among other things, the phase diagram at zero-temperature with density $\rho = 1$ using the density matrix renormalization group, and concluded that the anyons in 1D display insulator and superfluid phases. The first is characterized by having a nonzero energy gap in which the atoms are localized on the lattice, and the second by a gapless phase in which the atoms are delocalized and dispersed across the lattice. In addition, they presented the mean-field solution for the Mott-superfluid transition for different angles and a comparison with the bosonic case, where it is possible to see the expansion of the Mott lobes with the statistical angle. Later on, the ground-state properties of anyons in a one-dimensional lattice were analyzed by Tang *et al.* [30] using the Hamiltonian proposed by Keilmann *et al.* [29], and they obtained that anyons have an asymmetric quasi-momentum distribution, where the peak position depends on both the fractional phase and the particle number density. In the same way, the momentum distributions and the effects of the statistical angle on the correlations were analyzed using the density matrix renormalization group and mean field methods by Zhang *et al.*, finding that the statistical angle could modulate the beat length of the correlations [31].

In 2015, Greschner and Santos proposed an experimental scheme to improve the proposal for the realization of Keilmann's anyon-Hubbard model. This scheme allows as well for an exact realization of the two-body hard constraint (*i.e.* $(b_j^\dagger)^3 = 0$) and controllable effective interactions without the need for Feshbach resonances. They show that the interplay of anyonic statistics, two-body hard constraint, and controllable interactions results in a far richer physics for the model, and the phase diagram includes a pair-superfluid, a dimer, and an exotic partially-paired phase [32].

This year, a simple scheme for realizing the physics of 1D anyons with ultracold bosonic atoms in an optical lattice has been elaborated. It relies on lattice-shaking-induced resonant tunneling against potential off-sets created by a combination of a lattice tilt and strong on-site interactions. No lasers in addition to those used for the creation of the optical lattice are required [33]. Also, they calculated the density and the second Renyi entropy of a chain with twenty sites, using exact diagonalization.

Taking into account the above facts, it is clear that the anyon-Hubbard model is a very exciting problem, and we want to contribute to it. From the previous results, we know that the insulator regions grow as the statistical angle θ increases for density $\rho = 1$. In the present case, we are interested in the study of the influence of the increase in the density of the system on the position of the point at which the two phases separate. Furthermore, the mean-field solution for $\theta = \pi/4$ [29] indicates a possible odd-even asymmetry in which the insulator region with an even density increases in comparison with the lobes with odd densities. Hence we will study the system properties with $\theta = \pi/4$ to verify or challenge the mean-field results.

In this paper, we study the anyon-Hubbard model using the density matrix renormalization group (DMRG) method. Using the energy for adding and removing particles in the system, we construct the phase diagram for $\theta = \pi/4$ in the plane $(t/U, \mu/U)$ for three densities ($\rho = 1, 2, \text{ and } 3$) and we conclude that as we increase the density, the position of the critical point changes to lower values of kinetic energy t/U . These results contrast with previous mean-field calculations for $\theta = \pi/4$ [29]. On the other hand, it is necessary to find a tool that gives us a better estimate of the critical point than simply the gap closing. We consider that during the last decades, it has been shown that quantum information tools are useful for studying the border between the quantum phases [34]. In this system, the phase transition was studied using the block von Neumann entropy, and we were able to observe a critical and a noncritical behavior in the system related to the superfluid to Mott insulator transition. In particular, we use the estimator proposed by Läuchli and Kollath [35] to determine the critical points of the anyon-Hubbard model. We obtain the evolution of the critical points with the density and find functional relationships between the different parameters that the Hamiltonian depends on. We show that a simple analytical function is a good approximation of the results. It is important to note that studies related to the most precise estimation of critical points have not been previously reported, beyond the gap closing. We use the critical points and show that the Kosterlitz-Thouless formula is suitable for describing the closing of the gap, and we can infer that the anyon-Hubbard model with $\theta = \pi/4$ is in the same universality class as the Bose-Hubbard model.

The outline of this paper is as follows: In Sec. IA we introduce the anyon-Hubbard model. In sec. IB we show the phase diagram obtained and we study the critical

points of the system through the von Neumann block entropy. Finally, in Sec. IC we summarize our results.

A. Model

The anyon-Hubbard model takes into account the hopping of the anyons along the lattice and the local two-body interaction between them [29], and its Hamiltonian is given by

$$H = -t \sum_j^{L-1} (a_j^\dagger a_{j+1} + h.c.) + \frac{U}{2} \sum_j^L n_j (n_j - 1), \quad (1)$$

where $t > 0$ is the tunneling amplitude connecting two neighboring sites, U is the on-site interaction, L is the length of the lattice, n_j is the number operator and the operators a_j^\dagger , and a_j creates or annihilates an anyon on site j , respectively. The above creation and destruction operators satisfy the following commutation relation:

$$\begin{aligned} a_j a_k^\dagger - e^{-i\theta \text{sgn}(j-k)} a_k^\dagger a_j &= \delta_{jk}, \\ a_j a_k &= e^{i\theta \text{sgn}(j-k)} a_k a_j, \end{aligned} \quad (2)$$

where θ denotes the statistical phase, and the sign function is $\text{sgn}(j-k) = \pm 1$ for $j > k$ and $j < k$, and $= 0$ for $j = k$. Note that the bosonic commutation relations are reproduced at the same site ($j = k$). Thus two particles at the same site behave as ordinary bosons. In consequence, when $\theta = \pi$, we have pseudofermions: in spite of being bosons on-site, they are fermions off-site.

To study the ground state of the Hamiltonian (1), Keilmann *et al.* [29] proposed an exact mapping between anyons and bosons in 1D by means of the fractional version of a Jordan-Wigner transformation given by: $a_j = b_j \exp(i\theta \sum_{i=1}^{j-1} n_i)$, where the operator b_j describes spinless bosons, which satisfy $[b_j, b_i^\dagger] = \delta_{ji}$ and $[b_j, b_i] = 0$. The number operator is defined by $n_i = a_i^\dagger a_i = b_i^\dagger b_i$.

After using the anyon-boson mapping, the anyon-Hubbard Hamiltonian is given in terms of bosonic operators thus:

$$\begin{aligned} H &= -t \sum_j^{L-1} (b_j^\dagger b_{j+1} e^{i\theta n_j} + h.c.) \\ &+ \frac{U}{2} \sum_j^L n_j (n_j - 1). \end{aligned} \quad (3)$$

Note that the above Hamiltonian describes bosons with an occupation-dependent amplitude $te^{i\theta n_j}$ for hopping processes from right to left ($j+1 \rightarrow j$). If the target site j is unoccupied, the hopping amplitude is simply t . If it is occupied by one boson, the amplitude reads $te^{i\theta}$, for two bosons $te^{i2\theta}$, and so on. We fix the energy scales by considering $U = 1$.

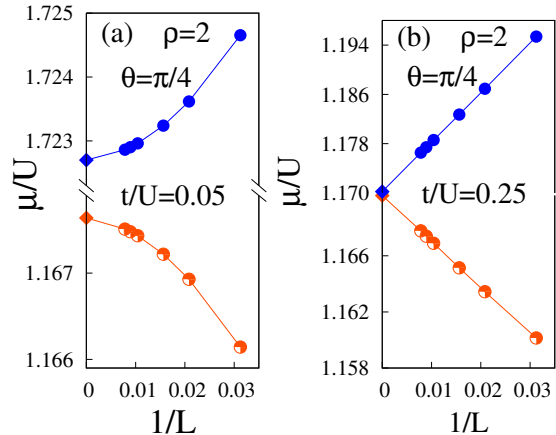


FIG. 1. (Color online) System size dependence of the chemical potential of anyons in 1D with statistical angle $\theta = \pi/4$ and $\rho = 2$. The upper set of data in each panel corresponds to the particle excitation energy and the lower one to the hole excitation energy. In the left panel ($t/U = 0.05$), we show a state with a finite difference at the thermodynamic limit, while this difference vanishes in the right panel ($t/U = 0.25$).

It is important to observe that, for $\theta = 0$ the anyon commutation relations revert to the well-known bosonic relations, and the anyon-Hubbard model corresponds to the well-known Bose-Hubbard model in this limit. Many analytical and numerical approaches have been used to study the ground state of the Bose-Hubbard model, and we know that for large t , the bosons would be completely delocalized in the lattice and the system would be in a superfluid state. When U dominates, an integer number of bosons would be localized at each site, and the ground state is a Mott insulator one. The border between the superfluid and the Mott insulator regions can be estimated with the energy for adding and removing particles:

$$\mu^p(L) = E_0(L, N+1) - E_0(L, N), \quad (4)$$

$$\mu^h(L) = E_0(L, N) - E_0(L, N-1), \quad (5)$$

where $E_0(L, N)$ denotes the ground-state energy for L sites and N particles. If the above parameters (L and N) are finite, we observe that the single-particle excitations exhibit a finite gap $\Delta\mu(L) = \mu^p(L) - \mu^h(L) = E_0(L, N+1) + E_0(L, N-1) - 2E_0(L, N)$. A Mott insulator state is achieved if the density of the system $\rho = N/L$ is an integer and is at the thermodynamic limit $\Delta\mu = \lim_{L, N \rightarrow \infty} \Delta\mu(L) > 0$. By contrast, the superfluid phase is gapless.

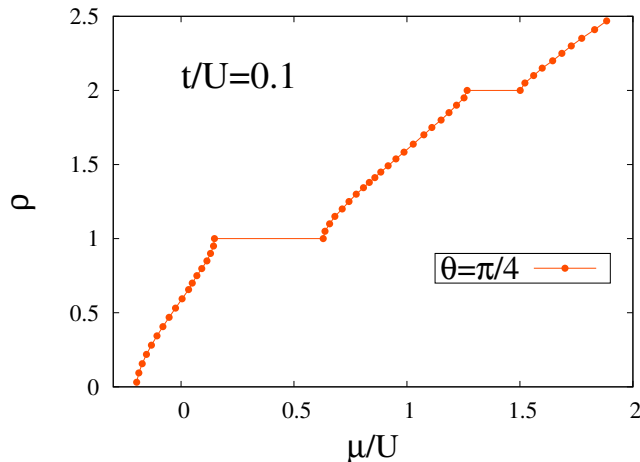


FIG. 2. (Color online) Density ρ versus chemical potential μ at the thermodynamic limit for $t/U = 0.1$ and a statistical angle $\theta = \pi/4$.

B. Results

To calculate the ground state of a lattice with L sites and N particles, we truncated the local Hilbert space by considering only $\rho + 5$ states when the density of the particles is ρ [36] and used the finite-size density matrix renormalization group algorithm (DMRG) with open boundary conditions. Also, we used the dynamical block state selection (DBSS) protocol based on a fixed truncation error of the subsystem's reduced density matrix instead of using a fixed number of preserved states in the DMRG sweeps [37]. Using this protocol, we obtained a discarded weight of around 10^{-9} or less, and the maximum number of states retained was $m = 1080$.

In the context of the quantum Hall regime, an experimental setup with a superconducting film adjacent to a two-dimensional electron gas can be understood in terms of anyons with a statistical angle $\theta = \pi/4$, and this system could prove useful in schemes for fault-tolerant topological quantum computation [38]. A mean-field calculation of the phase diagram of one-dimensional anyons for densities $\rho = 1, 2$, and 3 was presented by Keilmann *et al.* for $\theta = \pi/4$ [29]. The above facts motivated us to consider this special angle in the first part of our study.

The evolution of the energies for adding and removing particles given by Eq. 4 and Eq. 5 versus the inverse of the lattice length for anyons with $\theta = \pi/4$ and density $\rho = 2$ appear in Fig. 1. In each panel, the upper (lower) curve corresponds to the energy for adding (removing) particles. Regardless of the value of the hopping parameter, we obtained that the energy for adding (removing) particles always decreases (increases) as a function of $1/L$; however, this evolution is quadratic for $t/U = 0.05$, and at the thermodynamic limit we obtain $\Delta\mu/U = \lim_{L, N \rightarrow \infty} [\mu^p(L) - \mu^h(L)] = 0.55$, which suggests that the ground state corresponds to a Mott insulator one. On the other hand, for $t/U = 0.25$, the evo-

lution is linear, the energy for adding and removing particles meets at the thermodynamic limit, and the ground state is superfluid. This figure tells us that the anyon liquid passes from a Mott insulator state to a superfluid one when the kinetic energy increases; hence its behavior is similar to the Bose-Hubbard model ($\theta = 0$), and the main difference will be the position of the critical point.

In Fig. 2, we show the density ρ as a function of the chemical potential, which was found at the thermodynamic limit value. We observe that the chemical potential increases as the density grows; however this behavior changes when the density reaches integer values. For $\rho = 1$ and $\rho = 2$, we obtain two plateaus in the curve, which indicates that the ground state has a finite gap for integer densities, whereas the width of these plateaus give us the value of the gap. Comparing this with Fig. 1, we obtain that for a ground state with two bosons per site, the gap will decrease monotonously as the hopping parameter increases. An important fact in Fig. 2 is that the slope is always greater than zero, i. e. the compressibility $\kappa = \partial\rho/\partial\mu > 0$, an argument that is related to the absence of first-order transition. Note that Batrouni and his collaborators have shown the existence of first-order phase transitions ($\kappa < 0$) in two-dimensional system of spinless [39] and spinor [40] bosons, but for even lobes in one-dimensional systems of spin-1 bosons, the compressibility is positive and the phase transition is of first order, this being caused by the spin degree of freedom [41]. Taking into account the above discussion and our numerical results, we believe that the phase transitions for $\theta = \pi/4$ are of the second order kind; however the possibility of find first-order transitions in the anyon-Hubbard model for larger values of θ and/or a fixed number of particles is an interesting open problem.

The mean-field phase diagram of Hamiltonian (1) found by Keilmann *et al.* [29] is reproduced in Fig. 3 (gray squares). For $\theta = \pi/4$, we note that the Mott insulator lobes are surrounded by the superfluid phase, and their shapes are rounded. The mean-field solution shows that the critical points for all densities are lower than the ones found for the Bose-Hubbard model, and that the second lobe is larger than the other lobes. This result suggests a possible odd-even asymmetry present in the system in which lobes with an even density ($\rho = 2$) increase in comparison with those with odd densities ($\rho = 1$ and 3). In addition, we can see that the critical point for the densities $\rho = 1$ and $\rho = 3$ do not differ considerably.

Despite the interesting results of the mean-field solution of Hamiltonian (1), a determination of the phase diagram for higher densities ($\rho > 1$) beyond mean-field has not been done. For this reason, we calculated the chemical potential at the thermodynamic limit and found the phase diagram for $\theta = \pi/4$ and the three densities $\rho = 1, 2$, and 3 (blue line-circle) at the plane $(\mu/U, t/U)$. For small values of t/U , we see that the borders of the first Mott lobe obtained by mean-field and DMRG are closer; however for larger values the mean-field solution lobe closes, while the DMRG solution stretches slowly,

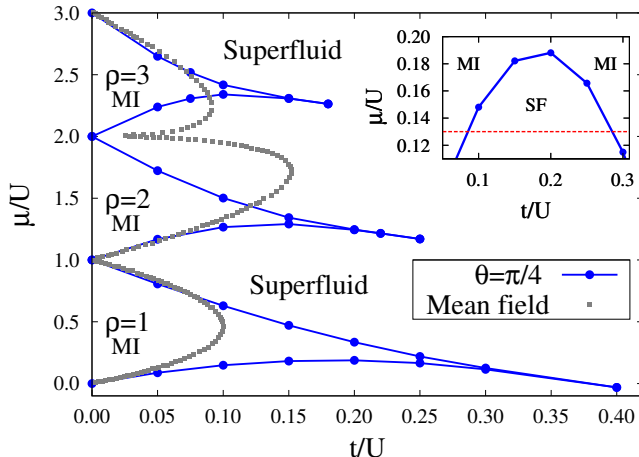


FIG. 3. (Color online) Phase diagram of the anyon-Hubbard model with statistical angle $\theta = \pi/4$ for the densities $\rho = 1, 2$, and 3 using DMRG (blue line-circle) and comparison with the mean-field solution (gray squares) for the same densities (mean-field data were taken from [29]). Inset: display sequence from Mott insulator to superfluid and back to Mott insulator for $\theta = \pi/4$ and $\rho = 1$ at fixed $\mu = 0.13$.

and the gap closes at around $t/U = 0.40$, which is four times larger than the mean-field result [see Fig. 3]. Note that our results are in agreement with the DMRG results of Keilmann *et al.* for $\rho = 1$. For the second lobe, we observe that the mean-field and DMRG solutions only coincide at the lower edge for small values of t/U . The area of the mean-field solution is greater and the DMRG gap closes at around $t/U = 0.25$, which indicates that there is no odd-even asymmetry between the lobes, this being an artifact of the mean-field solution. For the lobe with density $\rho = 3$, we obtain that the upper borders of both solutions are closer for small values of t/U and the critical point for this density is located around $t/U = 0.18$, which is lower than the location of the critical points for the other densities.

In Fig. 3, we observe that the area of the Mott insulator lobes decreases as the global density of the system increases, which implies that the location of the critical points moves to lower values with the density. These facts are consistent with those obtained for the Bose-Hubbard model [42]. However, the effect of anyonic statistics reflected in a correlated density dependent hopping is larger values of the critical points for all the densities considered, i. e., for a nonzero statistical angle, we need more kinetic energy to delocalize the particles and generate a superfluid state. Note that for all lobes, the gap closes as the hopping parameter increases and the shape of lobes becomes elongated, with a large tip, which indicates that the gap closes very slowly, a fact is relevant to determination of the type of phase transition.

In the inset of Fig. 3, we show a zoom of the lower edge of the first lobe and a chemical potential constant line ($\mu = 0.13$). Based on this inset, it is clear that the

hole excitation energy has a maximum value, a fact repeated for the others lobes, but the position of the maximum moves to lower values of the hopping. Moving on along the red line, we observe that for small values of t/U there is one boson per site, and the ground state is a Mott insulator one, but for bigger values a quantum phase transition takes place and the system passes to a superfluid phase with a global density lower than one. When $t/U \approx 0.28$, the system re-enters into a Mott insulator phase with density $\rho = 1$, and a new transition to a superfluid phase with global density greater than one is expected for larger values of the hopping. Note that this reentrance phase transition also happens for the other lobes calculated here. This fact was first discussed by Kuhner *et al.* for the Bose-Hubbard model ($\theta = 0$) with density $\rho = 1$ [43], and recently a detailed study was conducted by Pino *et al.* [44].

From the above discussion and the previous papers about the anyon-Hubbard model, we know that the ground state exhibits a Mott insulator phase and a superfluid phase whose boundaries were found here for three different densities considering an angle of $\theta = \pi/4$. However, to use the closing gap criterion to determine the critical point when the density is fixed is not appropriate, as has been widely discussed for the Bose-Hubbard model. The precise determination of the critical points of this last-named model has received significant attention in the last decade, and many approaches have been considered, for instance using the interaction parameter of the Luttinger liquid [42, 43], or the tools of quantum information theory [35, 45, 46]. Clearly, for the scientific community a precise determination of the critical points that separate the two quantum phases for the anyon-Hubbard model is a very interesting problem.

Today, entanglement is an important tool for studying the ground state of strongly correlated systems as well as the quantum phase transitions that will occur in the system. Measures of the entanglement, such as fidelity, von Neumann entropy, purity, and negativity, among others have been useful in determining the critical points of diverse models [34]. In the present paper, we will use the von Neumann block entropy for studying the ground state of the Hamiltonian (3).

We consider a system with L sites divided into two parts. Part A has l sites ($l = 1, \dots, L$), and the rest form part B , with $L - l$ sites. The von Neumann block entropy of block A is defined by $S_A = -\text{Tr} \varrho_A \ln \varrho_A$, where $\varrho_A = \text{Tr}_B \varrho$ is the reduced density matrix of block A and $\varrho = |\Psi\rangle\langle\Psi|$ the pure-state density matrix of the whole system. For a system with open boundary conditions, the behavior of the von Neumann block entropy as a function of l depends on the nature of ground state and provides information about the type of phase, because it saturates (diverges) if the system is gapped (gapless) [47], thus:

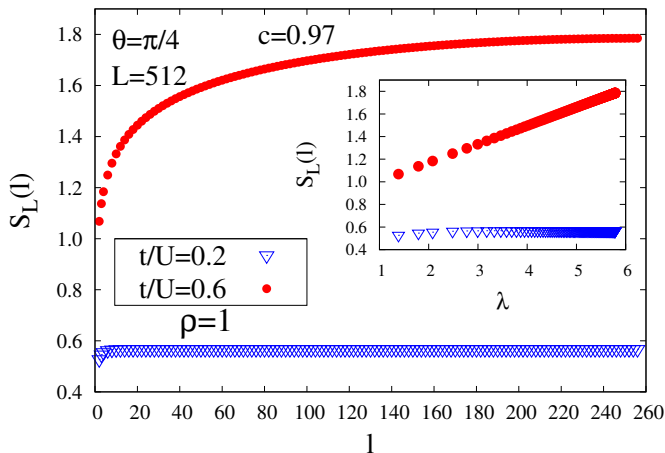


FIG. 4. (Color online) The von Neumann block entropy $S_L(l)$ as a function of l for a system with size $L = 512$, $\rho = 1$, and $\theta = \pi/4$. Here we consider two different values of the hopping parameter, $t/U = 0.2$ and $t/U = 0.6$. In the inset, the von Neumann block entropy $S_L(l)$ as function of the logarithmic conformal distance λ is shown, revealing a linear behavior for the critical state. Otherwise, the non-critical state does not exhibit linear behavior, because of the short correlation length. We found that the central charge is $c = 0.97$.

$$S_L(l) = \begin{cases} \frac{c}{6} \ln \left[\frac{2L}{\pi} \sin \left(\frac{\pi l}{L} \right) \right] + \Theta, & \text{critical,} \\ \frac{c}{6} \ln [\xi_L] + \Theta', & \text{non critical,} \end{cases} \quad (6)$$

where c is the central charge and ξ_L is the correlation length. The constants Θ and Θ' are nonuniversal and model dependent. The von Neumann block entropy $S_L(l)$ as a function of the block size l is shown in Fig. 4 for a lattice with global density $\rho = 1$, statistical angle $\theta = \pi/4$, and two different values of the hopping: $t/U = 0.2$ and $t/U = 0.6$. At the limit $t \rightarrow 0$, the ground state can be seen as a product of local states, i. e., it is separable, and we expected that the entanglement would be zero. For a nonzero value of the hopping $t/U = 0.2$, we observe that the block entropy is different from zero; it increases rapidly, and saturates at a certain value, in accordance with the expression Eq. (6), which indicates that the ground state has a finite correlation length, as is characteristic of the Mott insulator phase. A different behavior of $S_L(l)$ as a function of l is observed for $t/U = 0.6$; now the von Neumann block entropy always grows with the block size and diverges, which characterizes a critical state. In the inset of Fig. 4, we show the relationship between block entropy and the logarithmic conformal distance ($\lambda = \ln \left[\frac{2L}{\pi} \sin \left(\frac{\pi l}{L} \right) \right]$). We obtain a nonlinear dependence for small values of the hopping ($t/U = 0.2$) due to the short correlation length, and linear behavior is observed for the critical state ($t/U = 0.6$). Observing the expression (6), we note that the slope of the block entropy versus the logarithmic conformal distance is related

to the central charge of conformal theory; hence from the inset of Fig. 4 we obtain the central charge $c = 0.97$. This value is very close to 1, which corresponds to the central charge for the Bose-Hubbard model ($\theta = 0$). Specifically, in the superfluid phase the low-energy physics of the one-dimensional Bose-Hubbard model can be described as a Luttinger liquid, which is a conformal field theory with central charge $c = 1$ [35].

When the hopping increases from zero, the von Neumann block entropy allows us to identify two different ground states, one critical and the other not; however, identifying for which value of t/U the transition takes place is not an easy task. Nevertheless, we can calculate the block entropy for different values of t/U and try to estimate the critical value for which the system passes from a saturation behavior to a critical one, which could be a criterion for determining the critical point. In reality, this is very poor and needs a very large number of calculations. This problem was addressed by Läuchli and Kollath, who proposed an estimator in terms of the von Neumann block entropy defined by the following expression: $\Delta S(L) = S_L(L/2) - S_{L/2}(L/4)$. This measures the increase of the entropy at the mid-system interface upon doubling the system size [35]. According to (6), we obtain:

$$\Delta S_L(l) = \begin{cases} \frac{c}{6} \ln[2], & t \geq t_c, \\ 0, & t < t_c. \end{cases} \quad (7)$$

We expect that the behavior of ΔS will be a step function as a function of t/U . Even though other estimators have been proposed in the literature for determining the critical point using the block entropy [48], we follow the Läuchli and Kollath proposal, because it works well for the Bose-Hubbard model.

In Fig. 5, we show the dependency between the estimator ΔS_{LK} and t/U for $L = 256$ and $\rho = 1$ for two angles, $\theta = 0$ and $\theta = \pi/4$. The estimator is zero at $t = 0$ for any value of the statistical angle and remains constant in a finite region. The width of this region depends on the statistical angle, i. e. the width of the Mott insulator area will increase with the angle θ . The estimator grows quickly after a certain value of the hopping, which varies with the statistical angle and reaches the value $\ln(2)/6$. This value corresponds to the estimator evaluated in a critical region according to the expression Eq. (7). Note that the estimator remains constant at this value for larger values of the hopping. It is clear from the figure that the anyon-Hubbard model exhibits a Mott insulator and a superfluid phase and that the behavior of the estimator corresponds to a step function. The value of the critical point is taken as the first value to reach $\ln(2)/6$. In the inset of Fig. 5, we consider different system sizes, from 64 up to 512 sites, and observe that when the system size increases, the hopping for which $\Delta S_{LK} \neq 0$ moves to the right, and the curve tends to a step function as a function of t/U , and so we see that the expected behavior will occur.

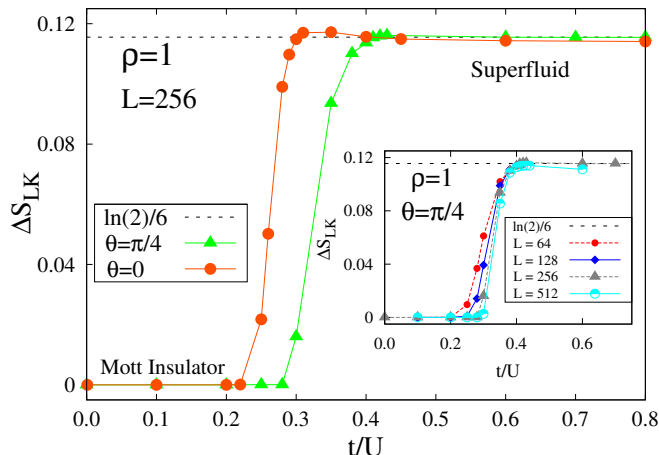


FIG. 5. (Color online) The estimator ΔS_{LK} as a function of the hopping parameter t/U for $\theta = 0$ and $\theta = \pi/4$. Here, we fixed $L=256$ and $\rho = 1$. In the inset, the estimator ΔS_{LK} vs t/U for $\theta = \pi/4$, and different system lengths $L = 64, 128, 256,$ and 512 . The lines are visual guides.

We found that the quantum critical point for $\theta = 0$ and $\theta = \pi/4$ are $t_c/U = 0.303$ and $t_c/U = 0.414$, respectively. Note that the result for the bosonic case $\theta = 0$ is in accordance with previous results [42]. It is important to observe that the most accurate determination of the critical point gives us a bigger value in comparison with the calculation shown in Fig. 3, where we observe that the gap closes at $t/U = 0.40$. The estimator results reinforce the idea that the inclusion of state-dependent hopping helps to localize the particles in this system; in other words, the inclusion of the correlated hopping means that the kinetic energy to delocate the system increases, since there is a displacement towards greater t/U of the critical point.

We have characterized the quantum phases of the anyon-Hubbard model with $\theta = \pi/4$, and we have shown that the use of the Läuchli and Kollath estimator allows us to better find the t_c/U position for the case $\rho = 1$. On the other hand, we showed that the central charge c in the critical phase is very close to 1. However, the kind of transition that is taking place has not yet been discussed. It is important to remember that for a fixed integer number of particles, the Bose-Hubbard model belongs to the universality class of the XY model; hence the gap closes following a Kosterlitz-Thouless formula [49]. We present the energy gap $\Delta\mu/U$ as a function of $(t_c - t)/U$ for anyon-Hubbard model with $\theta = \pi/4$ and for densities $\rho = 1$ and $\rho = 2$ in Fig. 6. We found the critical point for $\rho = 2$ following the same procedure used to determine the critical point for $\rho = 1$. Regardless of the density, we obtained that the gap exhibits a linear dependence for larger values of $(t_c - t)/U$; however, as the parameter diminishes, the gap decreases smoothly, and finally we observe that the gap vanishes very slowly, corroborating the results shown in Fig. 3. The above results obtained

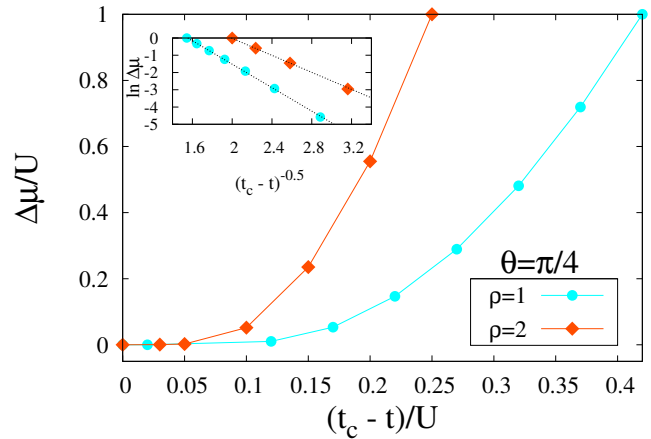


FIG. 6. (Color online) Energy gap as a function of $t_c - t$ for $\rho = 1$ and $\theta = \pi/4$. In the inset, $\ln \Delta\mu$ vs $1/\sqrt{t_c - t}$. Here, the points are DMRG results, and the fits to the Kosterlitz-Thouless transition are shown by lines.

for the anyon-Hubbard model suggest that we try to fit the curves in Fig. 6 to the Kosterlitz-Thouless formula:

$$\frac{\Delta\mu}{U} = \frac{\mu^p - \mu^h}{U} \sim \exp\left(\frac{\text{const.}}{\sqrt{(t_c - t)/U}}\right). \quad (8)$$

In the inset of Fig. 6, we present $\ln(\Delta\mu/U)$ as a function of $1/\sqrt{(t_c - t)/U}$, which shows a linear dependence for both densities. Therefore, we affirmed that the transitions are of the Kosterlitz-Thouless kind for these densities under the parameters considered. The above result and the fact that the central charge is close to 1 allow us to infer that the anyon-Hubbard model with $\theta = \pi/4$ is in the same universality class as the Bose-Hubbard model.

In Fig. 3, we show that the position of the critical points moves to lower values as the density increases. It is noteworthy that the functional dependency of the critical points of the superfluid-to-Mott-insulator transition with the density for the Bose-Hubbard was a problem addressed by Danshita *et al.* in 1D, 2D, and 3D [50]. They found that the critical values versus the density are well approximated by the function $\left(\frac{U}{D\rho t}\right)_c = a + b\rho^{-c}$, where D denotes the dimensionality of the system and the constants $a, b,$ and c are numerically determined. We wanted to find out whether the expression obtained by Danshita *et al.* is valid for the anyon-Hubbard model with $\theta = \pi/4$, so we increased the local Hilbert space, considering $\rho + 5$ states when the ground state with ρ particles per site is taken into account. This correction allows us to determine the critical points with more precision; however, the computational cost increases. Using the estimator (7) to find the critical points for higher densities, we obtain the results shown in Fig. 7 for a fixed value of the statistical angle ($\theta = \pi/4$) and its comparison with the bosonic case $\theta = 0$ (data taken from [50]). We can see how as the density increases, the position of the critical

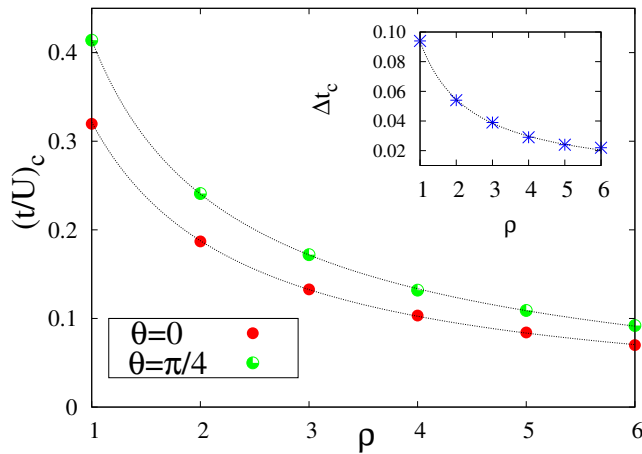


FIG. 7. (Color online) Quantum critical point position $(t/U)_c$ as a function of the density for the anyon-Hubbard model with $\theta = \pi/4$ and $\theta = 0$. The dashed lines represent the best fit of the numerical data with the function of Eq. (9). The numerical constants obtained for $\theta = \pi/4$ are $(\alpha, \beta, \gamma) = (-0.037, 0.45, -0.7)$ Inset: Δt_c between $\theta = 0$ and $\theta = \pi/4$ as a function of the density ρ . (the data of $\theta = 0$ were taken from [50])

point moves toward progressively smaller t values, which implies that the insulator region decreases as we increase the filling factor of the system. Within the interval of densities studied, the curve for anyons is above the curve for bosons. This implies that the Mott lobe is always greater for the anyon case. Nevertheless, as we increase the density, the difference between the critical points decreases.

The best fit of the numerical data of Fig. 7 was obtained using the relation

$$\left(\frac{t}{U}\right)_c = \alpha + \beta\rho^{-\gamma}, \quad (9)$$

with $\alpha = -0.037$, $\beta = 0.45$, and $\gamma = -0.7$ for the anyon case ($\theta = \pi/4$). Note that the above expression is different from the general formula found by Danshita *et al.*. We see in the inset of Fig. 7 the difference between the critical point positions of the Bose- and anyon-Hubbard model. This quantity decreases as the density grows and does not cancel out, which reflects the influence of the density-dependent hopping.

Due to the above mentioned motivation, we concentrated our study of the anyon-Hubbard model on the statistical angle $\theta = \pi/4$, but now we want to explore the evolution of the critical point position as a function of the angle, and so we consider larger values of the statistical angle, as is shown in Fig. 8. There, we present the results of the Läuchli and Kollath's estimator ΔS_{LK} as a function of t/U for a system with one boson per site and three different values of the statistical angle were considered. Regardless of the θ value, the behavior of the estimator is similar. We observe that it is zero in

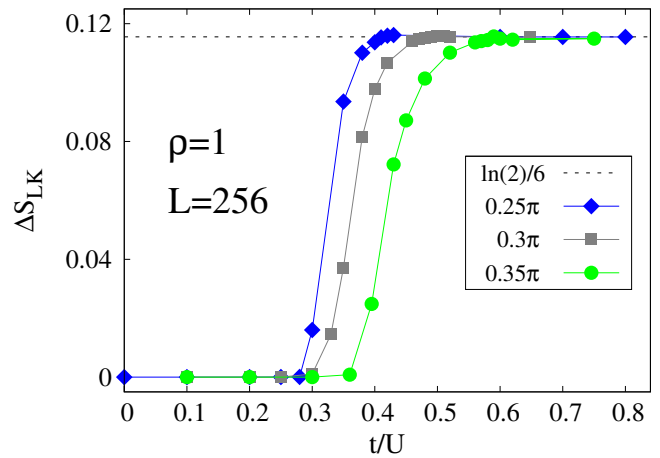


FIG. 8. (Color online) The estimator ΔS_{LK} as a function of the hopping parameter t/U for various statistical angles $\theta = 0.25\pi, 0.3\pi$ and 0.35π . Here, we fixed $L=256$ and $\rho = 1$.

a finite region of t/U values, indicating that the system is in a Mott insulator state in this region. Note that the size of this region increases with the angle in a non-linear proportion. After a certain value, which depends on the statistical angle, the estimator increases quickly and reaches the value of $(\ln 2)/6$. For larger values of t/U , the estimator remains constant at the latter value, which indicates that the system is in a superfluid state, in accordance with the expression Eq. (7). Although the results shown in this figure correspond to a lattice size of $L = 256$, we expected that for bigger lattices this behavior would be maintained, and a step function would be obtained in a manner similar to the inset of Fig. 5. On the other hand, we observe that the number of the states per block to reach the limit value $(\ln 2)/6$ increases dramatically with the statistical angle. From Fig. 8, we confirm that particles tend to localize when the statistical angle grows, a fact that is marked by an increase in the Mott insulator lobes area; therefore, the position of the critical point moves to larger values.

Using the vanishing gap criteria, Keilmann *et al.* estimate the evolution of the critical points as a function of the statistical angle for a global density $\rho = 1$, showing that critical strength U_c/t decreases with θ and vanishes at $\theta = \pi$ [29]. Today, we know that the above first approximation criterion is not very accurate, and taking into account that the Läuchli and Kollath estimator allows identify the border between the Mott insulator and the superfluid phases, we study the evolution of the critical points as the statistical angle increases in a chain with one or two particles per site (Fig. 9). We observe that the critical point increases gradually and smoothly with θ , regardless of the global density ρ , which reflects the increase in the localization of the particles. The effect of the repulsion between the particles is evident in Fig. 9, since for $\rho = 2$ more particles interact and the required kinetic energy to pass to the superfluid state is

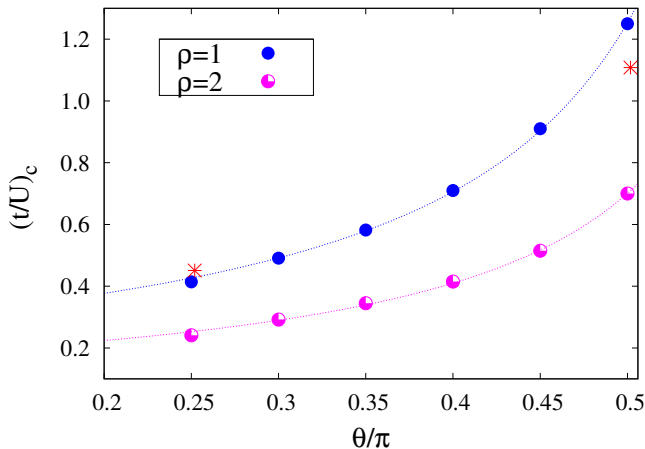


FIG. 9. (Color online) Critical point evolution with statistical angle θ for the anyon-Hubbard model. The dashed lines represent the best fit of the numerical data. The stars represent the critical points found by Keilmann *et al.*. We cannot explore larger values of θ due to the dramatic increase in the number of states that must be maintained in order to achieve the limit $(\ln 2)/6$.

less than for the $\rho = 1$ case for any value of θ . Note that the position of the critical points for $\rho = 2$ moves to greater values more slowly than in the $\rho = 1$ case as the statistical angle increases. When we compare the position of the critical points for the first Mott lobe found by Keilmann *et al.* with our results, we observe that for small (large) angles our critical point position moves to lower (greater) values compared to the Keilmann *et al.* results.

C. Conclusions

The ground state of the one-dimensional anyon-Hubbard model was studied, considering a mapping to

a modified Bose-Hubbard model, which was explored using the density matrix renormalization group method. We found that the anyon-Hubbard model exhibits two quantum phases: Mott insulator and superfluid. We presented a phase diagram for anyons with $\theta = \pi/4$ for the first three densities ($\rho = 1, 2$, and 3) and concluded that the density increase favors the appearance of the superfluid region, while the position of the critical point decreases. This result contradicts recently reported calculations of mean field theory and DMRG [31]. A reentrance phase transition was observed for the three densities. We calculated the evolution of the critical points with the density for $\theta = \pi/4$ and found an analytical expression $t_c/U = -0.037 + 0.45\rho^{-0.7}$ using the von Neumann block entropy and the estimator proposed by Läuchli and Kollath. For $\rho = 1$ and $\rho = 2$, we showed that the gap closing can be fit to a Kosterlitz-Thouless expression, and taking into account that the central charge is $c = 0.97$, we argued that the anyon-Hubbard model with $\theta = \pi/4$ belongs to the same universality class as the Bose-Hubbard model. We observed that the increase of the statistical angle leads to the localization of the particles, a fact that can be relevant when many-body interactions between particles are considered, because, for instance this can lead to obtaining Mott insulator phases for any density.

ACKNOWLEDGMENTS

The authors are thankful for the support of DIB-Universidad Nacional de Colombia and COLCIENCIAS (grant No. FP44842-057-2015). Silva-Valencia and Franco are grateful for the hospitality of the ICTP, where part of this work was done.

-
- [1] J. M. Leinaas and J. Myrheim, *Il Nuovo Cimento B* **37**, 1 (1977).
 - [2] F. Wilczek, *Phys. Rev. Lett.* **49**, 957 (1982).
 - [3] F. D. M. Haldane, *Phys. Rev. Lett.* **67**, 937 (1991).
 - [4] D. C. Tsui, H. Stormer, and J. Gossard, *Phys. Rev. Lett.* **48**, 1559 (1982).
 - [5] R. B. Laughlin, *Phys. Rev. Lett.* **50**, 1395 (1983).
 - [6] A. L. Fetter, C. Hanna, and R. Laughlin, *Phys. Rev. B* **39**, 9679 (1989).
 - [7] Y. H. Chen, F. Wilczek, E. Witten, and B. Halperin, *Int. Jour. Mod. Phys. B* **3**, 1001 (1989).
 - [8] B. I. Halperin, *Phys. Rev. Lett.* **52**, 1583 (1984).
 - [9] F. E. Camino, W. Zhou, and V. J. Goldman, *Phys. Rev. B* **72**, 075342 (2005).
 - [10] A. Y. Kitaev, *Ann. Phys.* **303**, 2 (2003).
 - [11] C. Nayak, S. H. Simon, A. Stern, M. Freedman, and S. D. Sarms, *Rev. Mod. Phys.* **80**, 1083 (2008).
 - [12] J. Alicea, Y. Oreg, G. Rafael, F. von Oppen, and M. P. A. Fisher, *Nat. Phys.* **7**, 412 (2011).
 - [13] A. Kundu, *Phys. Rev. Lett.* **83**, 1275 (1999).
 - [14] M. Batchelor, X.-W. Guan, and N. Oelkers, *Phys. Rev. Lett.* **96**, 210402 (2006).
 - [15] M. D. Girardeau, *Phys. Rev. Lett.* **97**, 100402 (2006).
 - [16] P. Calabrese and M. Mintchev, *Phys. Rev. B* **75**, 233104 (2007).
 - [17] C. Vitoriano, *Phys. Rev. Lett.* **102**, 146404 (2009).
 - [18] Y. Hao, Y. Zhang, and S. Chen, *Phys. Rev. A* **79**, 043633 (2009).
 - [19] Y. Hao and S. Chen, *Phys. Rev. A* **86**, 043631 (2012).
 - [20] N. T. Zinner, *Phys. Rev. A* **92**, 063634 (2015).
 - [21] O. I. Patu, *J. Stat. Mech.*, P01004 (2015).

- [22] B. Paredes, P. Fedichev, J. I. Cirac, and P. Zoller, *Phys. Rev. Lett.* **87**, 010402 (2001).
- [23] X. C. Xie, S. He, , and S. D. Sarma, *Phys. Rev. Lett.* **66**, 389 (1991).
- [24] L.-M. Duan, E. Demler, and M. D. Lukin, *Phys. Rev. Lett.* **91**, 090402 (2003).
- [25] L. Jiang, G. K. Brennen, A. V. Gorshkov, K. Hammerer, M. Hafezi, E. Demler, M. D. Lukin, and P. Zoller, *Nat. Phys.* **4**, 482 (2008).
- [26] M. Aguado, G. K. Brennen, F. Verstraete, and J. I. Cirac, *Phys. Rev. Lett.* **101**, 260501 (2008).
- [27] S. Longhi and G. D. Valle, *Optics Letters* **37**, 11 (2012).
- [28] Y. Zhang, G. J. Sreejith, and J. K. Jain, *Phys. Rev. B* **92**, 075116 (2015).
- [29] T. Keilmann, S. Lanzmich, I. McCulloch, and M. Roncaglia, *Nat. Commun.* **2**, 361 (2011).
- [30] G. Tang, S. Eggert, and A. Pelster, *New J. Phys.* **17**, 123016 (2015).
- [31] W. Zhang, E. Fan, T. C. Scott, and Y. Zhang, *arXiv:1511.01712* (2015).
- [32] S. Greschner and L. Santos, *Phys. Rev. Lett.* **115**, 053002 (2015).
- [33] C. Strater, S. C. L. Srivastava, and A. Eckardt, *ArXiv:1602.0838v1* (2016).
- [34] L. Amico, R. Fazio, A. Osterloh, and V. Vedral, *Rev. Mod. Phys.* **80**, 517 (2008).
- [35] A. M. Läuchli and C. Kollath, *J. Stat. Mech* , P05018 (2008).
- [36] J. Carrasquilla, S. R. Manmana, and M. Rigol, *Phys. Rev. A* **87**, 043606 (2013).
- [37] Ö. Legeza, J. Roder, and B. A. Hess, *Phys. Rev. B* **67**, 125114 (2003).
- [38] C. Weeks, G. Rosenberg, B. Seradjeh, and M. Franz, *Nat. Phys.* **3**, 796 (2007).
- [39] G. G. Batrouni and R. T. Scalettar, *Phys. Rev. Lett.* **84**, 1599 (2000).
- [40] L. de Forges de Parny, F. Herbert, V. G. Rousseau, and G. G. Batrouni, *Phys. Rev. B* **88**, 104509 (2013).
- [41] G. G. Batrouni, V. G. Rousseau, and R. T. Scalettar, *Phys. Rev. Lett.* **102**, 140402 (2009).
- [42] S. Ejima, H. Fehske, and F. Gebhard, *Europhys. Lett.* **93**, 30002 (2011).
- [43] T. D. Kühner, S. R. White, and H. Monien, *Phys. Rev. B* **61**, 12474 (2000).
- [44] M. Pino, J. Prior, A. Somoza, D. Jaksch, and S. Clark, *Phys. Rev. A* **86**, 023631 (2012).
- [45] S. Rachel, N. Laflorencie, H. F. Song, and K. L. Hur, *Phys. Rev. Lett.* **108**, 116401 (2012).
- [46] S. Ejima, H. Fehske, F. Gebhard, K. zu Munster, M. Knap, E. Arrigoni, and W. von der Linden, *Phys. Rev. A* **85**, 053644 (2012).
- [47] P. Calabrese and J. Cardy, *J. Stat. Mech* , P06002 (2004).
- [48] J. C. Xavier and F. C. Alcaraz, *Phys. Rev. B* **84**, 094410 (2011).
- [49] J. M. Kosterlitz and D. J. Thouless, *Journal of Physics C* **6**, 1181 (1973).
- [50] I. Danshita and A. Polkovnikov, *Phys. Rev. A* **84**, 063637 (2011).